Viscosities of Alcohol–Hydrocarbon Systems in the Critical Region: A Dynamic Laser Light Scattering Approach

R. R. Brunson* and C. H. Byers

Chemical Technology Division, Oak Ridge National Laboratory, Oak Ridge, Tennessee 37831-6224

The viscosities of pure alcohols and hydrocarbons, as well as binary mixtures of these compounds, were measured from room temperature to the critical region by use of a laser light scattering technique. Specially prepared monodispersed submicron silica particles were developed and used to achieve suspension stability into the critical region. The lower temperature data were verified by conventional techniques and by comparison with reliable literature data. In both pure materials and mixtures, the Andrade correlation is clearly not applicable over a wide temperature range. Excess viscosity indicates expected disruption of hydrogen-bonding networks by the hydrocarbons in alcohols.

Introduction

Dynamic light scattering commonly has been used to size particles in a liquid, but this method of characterizing particles also permits one to extract information concerning the physical properties of the liquid containing the particles. If monodispersed particles are diffused in a Brownian manner, then the scattered light from these particles will reveal the mobility of the particles. This particle mobility is a function of particle size and fluid viscosity; therefore, if the particle size is known, the viscosity of the suspending fluid can be related to the mobility parameters of the particle. Basically, this method of viscosity measurement is the inverse of a particle sizing method that has become widely accepted in microbiology and in polymer and colloid sciences (*1*, *2*).

Since conventional methods of measuring viscosity at elevated temperatures are impractical and inaccurate, few compounds have been investigated above their normal boiling points. Past light scattering studies demonstrated that a dynamic light scattering approach to viscosity measurement can be a valuable analytical tool when the temperature of a liquid is near or above its boiling point (*3*). The dynamic light scattering method offers a system that gives rapid and relatively safe high-temperature viscosity measurements. The system is nonintrusive on the sample, uses small sample volumes, and has a simple containment for samples.

The study of alcohols and alcohol–hydrocarbon systems is of particular interest from several viewpoints. First, the method with which we are dealing requires that suspensions of submicron particles remain stable throughout the temperature range of interest. The hydrocarbons and alcohols represent two important classes of materials which provide an important test of the suspension technology. Second, from a fundamental point of view, the mixture viscosities of these two classes of materials gives an interesting insight into the effect the hydrocarbon has upon the hydrogen-bonding network of the alcohol. Finally, mixture data for all such systems are not generally available between the normal boiling point and the critical point, so some data are needed to explore the theoretical implications of this region.

* Author to whom correspondence should be addressed.

Theoretical Background

The scattered light from a dilute colloidal suspension in a transparent liquid is related to the physical properties which cause the fluctuations of the solution and the scattering disposition. The physical phenomenon that governs the behavior of dilute colloidal suspensions is Brownian motion. Brownian motion can be observed in particles that are relatively large (1-μm diameter) on the molecular scale (*1*, *4–6*).

Brownian motion of a free particle (i.e., no applied force field) is described by the Langevin equation (*4*):

$$d\bar{u}/dt = -\beta\bar{u} + \bar{A}(t) \tag{1}$$

where $\bar{u}$ = particle velocity vector, t = time, β = coefficient of dynamic friction, and $\bar{A}(t)$ = fluctuating influence of molecular collision process.

For a spherical particle, the coefficient of dynamic friction is given by Stokes' law:

$$\beta = 6\pi a\eta/m \tag{2}$$

where α = particle radius, η = fluid viscosity, and m = mass of particle.

A detailed theoretical formulation of the solution to the Langevin equation and how it is used in relating the particle motion to light signal fluctuations is given elsewhere (*1*). This derivation yields an equation for a system of monodispersed colloidal particles:

$$A_s^* \approx \exp(-q^2Dt) = \exp(-t/\tau_c) \tag{3}$$

where $q = |\bar{q}| = 4\pi n[\sin(\theta/2)]/\lambda_l$, D = diffusion coefficient $= kT/(6\pi a\eta)$, k = Boltzmann constant, T = absolute temperature, K, and τ_c = characteristic decay time $= (q^2D)^{-1}$.

For polydispersed systems, the equation that results is

$$A_s^* = K\int_{r=0}^{r=\infty}[f(r)\,P(q,r)r^6\exp(-t/\tau_l)]\,dr \tag{4}$$

where r = particle radius, $f(r)$ = normalized distribution of particle size, $P(q,r)$ = Mie scattering factor, $P \approx 1$ for $r \ll \lambda$, and τ_l = decay time for $r = r_l$.

The exact solution requires inversion of this equation to yield $f(r)$ directly, but this is very difficult to do accurately for complex signals. However, significant improvements have been made in the development of a computer algorithm to deconvolute this integral (*7*). The r^6 dependence of the scattering power indicates that large particles are more easily detected than small ones.

A method of cumulants is a widely used technique for detecting polydispersity (*8–10*). This analysis leads to an approximation for the autocorrelation function:

$$\ln(A_s) = -\bar{\Gamma}t + \frac{\mu_2 t^2}{2!} - \frac{\mu_3 t^3}{3!} + \ldots$$

$$= -\bar{\Gamma}t + \frac{1}{2!}\frac{\mu_2}{\bar{\Gamma}^2}(\bar{\Gamma}t)^2 - \frac{1}{3!}\frac{\mu_3}{\bar{\Gamma}^3}(\bar{\Gamma}t)^3 + \ldots \tag{5}$$

The form of $\ln(A_s^*)$ is a polynomial in t with the coefficients representing different properties of the line-width distribution.

0021-9568/89/1734-0046$01.50/0

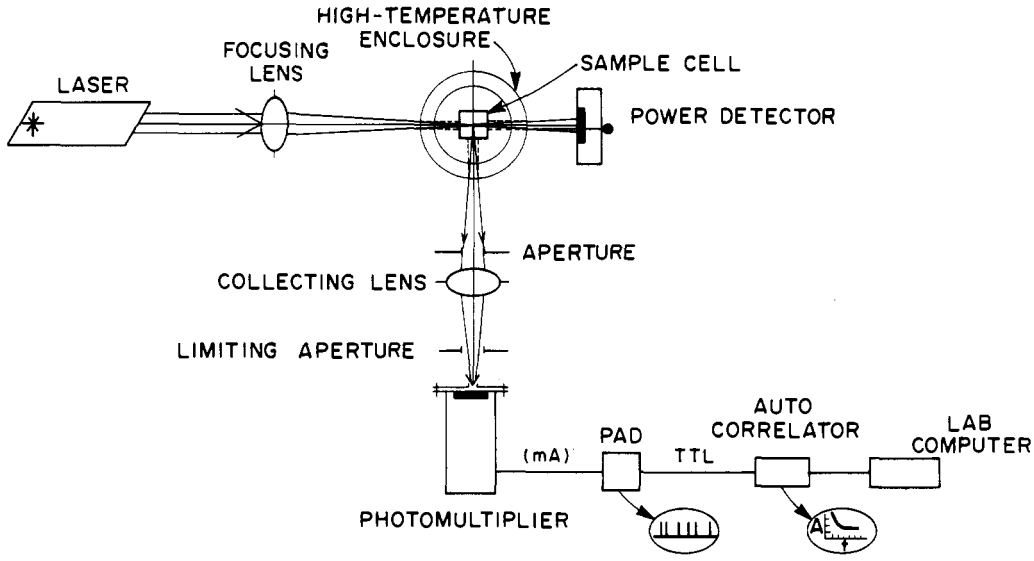

Figure 1. Dynamic laser-light-scattering spectrometer for viscosity measurements at high temperature and pressure.

The linear and quadratic terms, which are the most significant, are readily measured in most experiments. The linear term is the average line width as defined in eq 5. Since the scattering power of individual particles is skewed heavily toward large particles (eq 3), this "average" Γ will result in "average" diameters weighted toward the largest species.

The second moment (μ_2) normalized by the square of the average line width ($\mu_2/\bar{\Gamma}^2$) is termed the polydispersity parameter. For a perfect monodisperse suspension, $\mu_2/\bar{\Gamma}^2 = 0$. In practice, values of $\mu_2/\bar{\Gamma}^2$ less than -0.1 are taken as an indication of a narrow distribution.

It is readily apparent that a quadratic regression analysis of ln $[A_s^*(t)]$ versus t will provide estimates of $\bar{\Gamma}$ and $\mu_2/\bar{\Gamma}^2$. Using the Stokes–Einstein relation, we obtain the viscosity directly, since

$$D = \bar{\Gamma}/(2q^2) \tag{6}$$

and

$$d_p = kt/(3\pi\eta D) \tag{7}$$

As we indicated in an earlier publication, the excess viscosity (μ_E) may be defined as

$$\mu_E = \mu_{mix} - \mu_{mix}^{\circ} \tag{8}$$

where μ_{mix}° is the mixture viscosity of an ideal solution of the same concentration (*11*). Tests on binary mixtures displaying thermodynamic ideality led to the equation

$$\mu_{mix}^{\circ} = (x_1\mu_1^{1/3} + x_2\mu_2^{1/3})^3 \tag{9}$$

Deviations of ideal mixtures from this formula were generally less than 3%; therefore, eq 9 provides a useful benchmark for comparison with results from real mixtures. Negative values for excess viscosity indicate some intermolecular repulsion or the breaking of bond networks, while positive values are attributed to attraction or even bond formation between the two species. Since the hydrocarbon in alcohol–hydrocarbon mixtures tends to reduce hydrogen bonding in the alcohol, it is anticipated that negative deviations will prevail here.

Experimental Section

Apparatus. A custom-built, dynamic light scattering spectrometer was the centerpiece of this experiment. The apparatus (Figure 1) consists of (1) a laser, (2) source optics, (3) sample enclosure, (4) collection optics, (5) detector, and (6) signal processing equipment. Except for the high-temperature enclosure, the specification and assembly of components were based on established guidelines (*2*, *6*). The high-temperature enclosure was designed specifically for this study.

A 2-W argon ion laser (Spectra Physics Model 165-06) generates a vertically polarized beam (λ = 488 nm) that was focused onto the center of a standard quartz spectrophotometer cuvette which contains the sample. The beam was focused to a narrow (0.2 mm) width in order to maximize the modulation of the scattered light (i.e., high signal/noise). Typically, only low-power operation (<100 mW) was necessary.

The high-temperature enclosure (*12*) provides for temperature control of the sample to 500 °C and pressurization to 7 MPa. The body of the enclosure is a 7.6 × 7.6 × 10.1 cm stainless steel block. Quartz windows (Bond Optics, OPTISIL-3; 2.5-cm-o.d. × 1.9-cm-thick, 40-20 finish) act as ports for the incident beam, the transmitted beam, and the light scattered at 90°. A top flange permits access to the sample cell, facilitates pressurization, and allows direct measurement of the fluid temperature (type K thermocouple). The top and window flanges seal against O-rings. The entire block is insulated to minimize heat losses and thermal gradients.

The block temperature is maintained to within 0.1 °C of the set point by a PI-time proportioning controller. The controller operates a power relay that supplies adjustable voltage to four 100-W cartridge heaters. A regulated argon gas cylinder provides the overpressure needed for high-temperature measurements. Earlier studies with similar substances have shown that the dissolution of argon into the fluid phase has a negligible effect upon the sample viscosity in the range of this study (*12*).

The collection optical system limits the light reaching the detector to that scattered at 90° from a small volume (0.2 × 0.2 × 0.2 mm). Guidelines for the sizing and placement of the limiting apertures have been reviewed in several articles (*1*, *2*, *6*). The first aperture is a small iris diaphragm (0.68 mm; Ealing No. 22-3305) located just in front of the imaging lens. A 100-mm, plano-convex lens is placed approximately 20.3 cm from the center of the sample cell. The final aperture is a precision adjustable slit mounted vertically, just in front of the detector and in the plane of the image formed by the lens. All of the components are positioned along the axis normal to both the incident beam and the plane of polarization. The detector is an end-window photomultiplier (EMI No. 9863B350) mounted in a housing that provides radio-frequency and magnetic shielding (Pacific Model 3262 RF). A pulse amplifier discriminator (PAD, Langley Ford Model 1096) converts the milliampere pulses generated by the photomultiplier tube (PMT) to TTL

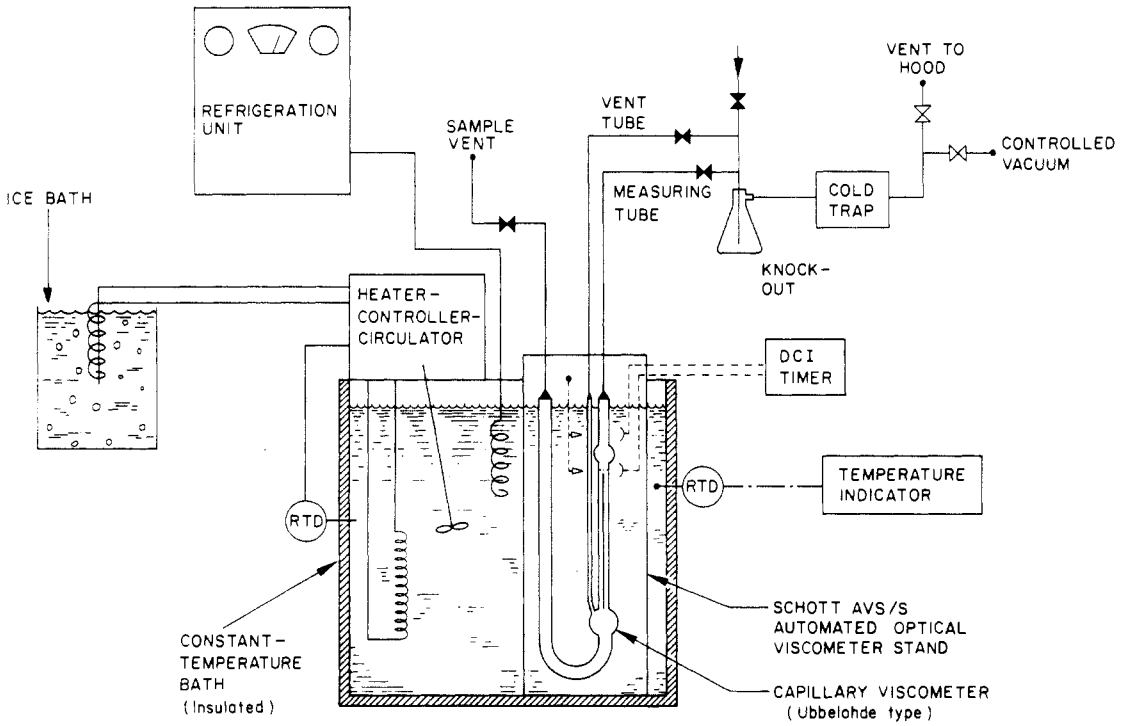

Figure 2. Capillary viscometer system used for low-temperature measurements.

pulses (0–5 V dc) for use in a sophisticated digital correlator (Langley Ford model 1096). This digital signal processor accurately approximates ideal autocorrelation functions. An RS-232 communications interface between the autocorrelator and a microcomputer permits automated operation, off-line analysis, and convenient data logging. The custom-built dynamic light scattering spectrometer is described in detail in a previous paper (*13*).

A conventional method of measuring the viscosity of fluids was also employed in this study to give reference viscosities for the pure components and their mixtures at temperatures below the boiling points. The apparatus (Figure 2) used for this conventional method is detailed in a previous paper (*13*). The major component is a glass Ubbelohde viscometer. The experimental equipment also included a constant-temperature bath and a piping system for drawing samples into the capillary tube. A calibrated, platinum, resistance thermometer connected to a digital Fluke RTD sensor (Model 2180A) made it possible to measure temperatures accurately to within 0.1 K. The entire experimental unit (except readout devices) was covered and heavily insulated to minimize temperature gradients. Liquid efflux time was determined electronically with fiber optic detectors with an accuracy of 0.01 s, essentially removing one of the persistent sources of experimental error in older devices. The operation and theory of capillary viscometers are discussed extensively in the literature (*6*, *13*, *14*).

The viscometers used in this conventional method relate the efflux time, t, to the kinematic viscosity ν as

$$\nu = \mu/\rho = K_C\Delta t - K_E/\Delta t^2 \qquad (10)$$

where the calibration constant K_C is expressed as

$$K_C = \left(\frac{\pi}{8}\right)\left(\frac{\bar{z}R^4}{L\,\Delta V}\right) \qquad (11)$$

and K_E is the kinetic energy correction constant. The manufacturer's (Schott Gerate) calibration values were confirmed in our laboratory with both water and toluene as calibrating fluids.

To obtain the dynamic viscosity μ it is necessary to determine the density of the fluid at the temperature of the experiment. As was reported in a previous paper, the densities of all of the mixtures were measured by using calibrated pycnometers to an experimental accuracy of 0.3%. On the basis of the findings of our previous studies (*11*, *15*), densities of pure components may also be predicted by the method of Gunn and Yamada (*16*). The specific volume of a pure saturated liquid is given as a function of temperature, given critical data, acentric factor, and density data at one temperature in addition to the critical point. Data used to calculate densities for all the components in this study are those tabulated by Reid, Prausnitz, and Sherwood (*17*). The liquids used in this study are chemically similar, and the pressure is low, so it is appropriate to select Amagat's law as a mixing rule. The molar volume of the mixture is given as

$$V_m^L = \sum_j x_j V_j^L \qquad (12)$$

where x_j is the mole fraction of component j, and V_j^L is the molar volume of the pure components. This rule should be quite accurate for all mixtures in the study.

The refractive indices of the fluids at elevated temperatures were calculated according to the standard Eykman equation (*18*). The accuracy of this estimation method is >99% and has been used in a previous study (*13*). This study also employed an ABBE 60 Refractometer to verify the estimated refractive indices of the fluids up to their boiling points. A Bausch & Lomb monochromator provided the correct light wavelength.

Preparation of Organophilic Sols. In order to interpret our light scattering results, we must deal with systems that conform to relatively ideal models. Central to the technique proposed in this report is the nature of the seed particles added to the fluids whose viscosities are to be determined. It is important to use seed particles as monodispersed as possible in order to avoid the complications associated with the analysis of systems having extreme size distributions. The particles must also be physically and chemically stable at the conditions of interest. Finally, the seed should exhibit stability against aggregation and must conform to the assumptions inherent in the Stokes–Einstein equation (eq 7). A seed that fulfills these requirements will form a model organophilic sol in nonpolar organic fluids. A

number of different methods were tested for the preparation of organophilic sols, but the synthesis suggested by Van Helden was most successful (*19*). The particles produced by this method meet all the requirements mentioned previously, and the method is relatively simple.

The preparation suggested by Van Helden is actually a combination of an alcohol preparation, such as that developed by Stober, and a surface treatment, such as that of Iler (*20*, *21*). A monodisperse silica sol is formed by the controlled hydrolysis of tetraethyl orthosilicate [$Si(OC_2H_5)_4$] in an alcohol–ammonia–water mixture. The silica particles are rendered organophilic by chemically bonding stearyl alcohol [$CH_3(CH_2)_{17}OH$] to the particle surface. The resulting particles form stable colloidal suspensions in a number of nonpolar aliphatic, cyclic, and aromatic solvents. This technique apparently eliminated problems which were experienced by other workers with charges on the particle surfaces.

Tetraethyl orthosilicate (TEOS) is hydrolyzed in the presence of water, with ammonia acting as a catalyst. In a typical preparation, 5.4 mL of concentrated NH_4OH (28% NH_3) is mixed with 85 mL of absolute ethanol in a clean flask. The TEOS is added (3.54 g) and the reaction mixture is stirred at constant temperature (25 °C) for at least 4 h. Our standard procedure generally results in spherical particles of 0.1 mm diameter. The size of the particles can be controlled by varying the reactant concentrations. The alcosol particles are stabilized by electrostatic forces and remain in suspension for months.

Five grams of stearyl alcohol, along with 100 mL of ethanol, are added to the alcosol as a slurry. The ethanol addition allows the water to be easily removed by shifting the water content below the azeotropic composition. After distillation of the ethanol and water at atmospheric pressure, a nitrogen blanket is introduced. The silica–stearyl alcohol mixture is heated to 190 °C and maintained at that temperature for at least 3 h to complete the esterification reaction between the silica and the stearyl alcohol, forming a Si–O–C linkage to the particle surface.

The modified silica is separated from the excess stearyl alcohol by sequential centrifugation. For the first separation, a 60/40 (v/v) mixture of chloroform and cyclohexane is added to the mixture. Chloroform is an excellent solvent for the excess stearyl alcohol, while cyclohexane lowers the density enough to make centrifugation of SiO_2 practical. The supernate is discarded and the process repeated with the solvent of interest. Before centrifugation, sonication of the suspension is sometimes necessary to redisperse the particles and ensure good contacting. Normally only three cycles are necessary to produce dispersions free of contaminants. High-quality reagents (>99%) are used without further purification.

Light Scattering Measurements. The organophilic preparation results in a fairly concentrated stock suspension which is then diluted with pure reagent to reduce the particle concentration. Particle interaction effects are minimized by diluting to concentrations of <50 ppm solids. A preliminary light scattering test using a low-temperature, low-power spectrometer (Langley Ford Model LSA-6) is used to determine the particle concentration that will provide sufficient signal strength. The optics of this unit are fixed at a scattering angle of 90°. Preliminary tests also help screen out samples that do not justify further study.

We followed the recommendations of Degiorgio and Lastokova for the operation of the digital correlator (*22*). The sample time is selected so as to span about four decay times. Laser power and aperture settings are adjusted to provide good signal/noise ratios (coherent scattering) and strong signals. A number of short (60-s) independent runs are superior to one long run, since the average of the runs provides a more accurate estimate of the viscosity, and the standard deviation provides information about the measurement's reproducibility. With optimized operation and a stable sample, five replicate runs (60 s each) yielded a coefficient of variation of the predicted viscosity of <1%.

Once the sample cuvette is aligned in the high-temperature enclosure, a base-line diameter is obtained at ambient conditions. This diameter is calculated on the basis of a predetermined low-temperature viscosity and is used in subsequent viscosity calculations. Measurements at higher temperatures are conducted only after the sample has thermally equilibrated with the enclosure (15 min at temperature). High-temperature refractive indices are calculated according to the standard Eykman equation (*18*). The accuracy of this estimation method is >1%. An argon overpressure of at least 50% of the saturation pressure is applied for measurements conducted above the normal point. Finally, after cooling, additional measurements are made at ambient conditions to check the stability of the sol. The initial and final diameter results should correspond within ±2%.

Table I. Capillary Viscosity Data for Pure 1-Butanol

temp, K	ν, mm^2/s	μ, mPa·s	ρ, kg/L	%CV[a]
291.5	3.754	3.046	0.8115	0.48
294.5	3.471	2.806	0.8085	0.01
298.5	3.129	2.517	0.8044	0.02
300.5	2.972	2.385	0.8023	0.02
307.6	2.502	1.989	0.7951	0.02
314.6	2.121	1.671	0.7878	0.04

[a] Coefficient of variation for set of runs = (standard deviation/mean) × 100.

Table II. Laser Light Scattering Viscosity Data for Pure Ethanol

temp, K	μ, mPa·s	ρ, kg/L	temp, K	μ, mPa·s	ρ, kg/L
293.7	1.160	0.7882	393.2	0.320	0.6646
294.1	1.137	0.7877	393.2	0.312	0.6646
294.5	1.171	0.7873	411.7	0.216	0.6383
295.4	1.158	0.7862	411.7	0.215	0.6383
298.2	1.068	0.7830	413.2	0.221	0.6361
298.2	1.077	0.7830	413.2	0.220	0.6361
308.2	0.911	0.7714	417.8	0.174	0.6294
308.2	0.915	0.7714	417.8	0.172	0.6294
308.2	0.926	0.7714	433.2	0.166	0.6061
318.2	0.805	0.7597	433.2	0.165	0.6061
318.2	0.797	0.7597	442.2	0.132	0.5921
318.2	0.822	0.7597	442.2	0.132	0.5921
338.2	0.628	0.7358	453.2	0.137	0.5746
338.2	0.626	0.7358	453.2	0.139	0.5746
343.2	0.584	0.7297	463.2	0.106	0.5583
343.2	0.583	0.7297	463.2	0.106	0.5583
348.2	0.529	0.7235	473.2	0.096	0.5417
348.2	0.529	0.7235	473.2	0.096	0.5417
358.2	0.482	0.7110	483.2	0.090	0.5249
358.2	0.486	0.7110	493.2	0.078	0.5078
368.2	0.407	0.6982	493.2	0.077	0.5078
373.2	0.405	0.6916	493.2	0.079	0.5078
373.2	0.404	0.6916	498.2	0.075	0.4992
378.0	0.354	0.6853	503.2	0.069	0.4906
392.2	0.291	0.6660			

Results and Discussion

Pure Component Viscosity Data. Viscosities of three pure compounds for which data are available over a significant temperature range were measured. These fluids include ethanol, 1-butanol, and *n*-heptane. To verify the precision of our laser light scattering results, low-temperature viscosity data were measured and compared with literature data in the cases of ethanol and *n*-heptane (*23*, *24*). In the case of 1-butanol, a measurement with a capillary viscometer was used for comparison and verification (Table I). Details of the measurement

Table III. Laser Light Scattering Viscosity Data for Pure 1-Butanol

temp, K	μ, mPa·s	ρ, kg/L	temp, K	μ, mPa·s	ρ, kg/L
292.5	2.905	0.8104	343.3	1.002	0.7579
292.5	3.060	0.8104	343.3	1.010	0.7579
292.7	2.933	0.8102	343.3	1.002	0.7579
292.9	3.009	0.8100	374.6	0.519	0.7242
303.3	2.227	0.7994	382.8	0.287	0.7150
303.3	2.227	0.7994	383.8	0.217	0.7139
323.9	1.470	0.7782	398.4	0.158	0.6972
323.9	1.464	0.7782	423.7	0.114	0.6668
323.9	1.470	0.7782			

Table IV. Laser Light Scattering Viscosity Data for *n*-heptane

temp, K	μ, mPa·s	ρ, kg/L	temp, K	μ, mPa·s	ρ, kg/L
292.1	0.426	0.6838	348.8	0.232	0.6345
293.1	0.423	0.6838	353.1	0.214	0.6305
293.1	0.419	0.6838	353.1	0.216	0.6305
293.1	0.412	0.6838	363.1	0.197	0.6211
298.4	0.369	0.6792	363.1	0.199	0.6211
298.4	0.362	0.6792	373.1	0.201	0.6110
303.1	0.347	0.6752	376.4	0.179	0.6083
303.1	0.343	0.6752	399.4	0.163	0.5851
313.1	0.309	0.6665	400.9	0.148	0.5835
323.1	0.270	0.6577	401.0	0.146	0.5834
323.1	0.278	0.6577	423.0	0.123	0.5596
333.1	0.252	0.6488	423.1	0.124	0.5590
343.1	0.234	0.6397	423.7	0.128	0.5580
348.5	0.231	0.6348	448.2	0.131	0.5304

Table V. Capillary Viscosity Data for Ethanol–*n*-Heptane System

x(EtOH)	temp, K	ν, mm²/s	μ, mPa·s	ρ, kg/L	%CV[a]
0.3	294.4	0.667	0.466	0.6981	0.62
	297.2	0.645	0.448	0.6955	0.85
	300.5	0.621	0.430	0.6925	0.68
	303.6	0.598	0.412	0.6898	0.17
0.5	303.2	0.695	0.489	0.7043	0.52
	313.2	0.612	0.425	0.6948	0.18
	323.3	0.548	0.375	0.6850	0.50
	328.1	0.522	0.355	0.6804	0.75
	338.2	0.477	0.320	0.6704	1.67
0.8	293.8	1.126	0.842	0.7482	2.29
	297.3	1.098	0.818	0.7444	1.71
	303.3	0.951	0.702	0.7382	0.38
	308.9	0.878	0.643	0.7323	1.04
	313.4	0.819	0.596	0.7276	0.60
0.9	293.2	1.300	0.996	0.7659	1.21
	298.2	1.186	0.902	0.7605	0.86
	300.8	1.132	0.858	0.7577	0.77
	306.2	1.043	0.784	0.7518	0.56
	308.2	1.008	0.756	0.7496	0.20

[a] Coefficient of variation for set of runs = (standard deviation/mean) × 100.

method are given elsewhere (*15*).

Laser light scattering viscosity measurements were made for all three compounds from room temperature to the highest temperature at which the silica suspension was stable for the particular material. Results for ethanol, *n*-heptane, and 1-butanol are given in Tables II, III, and IV, respectively. Ethanol formed the most stable suspension, remaining intact to within 13 °C of the critical point. An independent mechanical failure prevented the acquisition of data above 230 °C. The other two materials, while less stable, remained usable well above the normal boiling point. Two key factors could lead to greater stability: the production of smaller silica particles and the use of stearic acid homologues as the bridging material bonded to the silica. These factors are under investigation. The results for ethanol are shown in Figure 3 in terms of an Arrhenius plot. Our data significantly extend the data available in the literature and agree with the existing data over a broad temperature

Table VI. Laser Light Scattering Viscosity Data for Ethanol–*n*-Heptane System

x(EtOH)	temp, K	μ, mPa·s	ρ, kg/L
0.3	294.1	0.461	0.6984
	294.0	0.463	0.6985
	294.2	0.463	0.6983
	304.4	0.409	0.6891
	314.9	0.363	0.6786
	325.6	0.323	0.6696
	344.1	0.269	0.6522
	362.5	0.222	0.6342
	379.2	0.192	0.6173
	384.0	0.180	0.6123
	400.6	0.159	0.5945
	402.6	0.151	0.5923
	417.8	0.136	0.5751
	431.3	0.120	0.5593
	463.3	0.094	0.5192
	473.8	0.090	0.5053
	492.0	0.076	0.4806
	492.4	0.077	0.4800
0.5	295.3	0.549	0.7118
	295.6	0.544	0.7115
	295.6	0.548	0.7115
	303.2	0.482	0.7043
	315.2	0.404	0.6929
	354.2	0.277	0.6545
	372.2	0.233	0.6358
	395.2	0.189	0.6106
	404.2	0.173	0.6003
	434.2	0.163	0.5640
	434.7	0.265	0.5633
	458.9	0.260	0.5318
0.8	293.4	0.868	0.7481
	294.4	0.852	0.7471
	294.4	0.848	0.7471
	307.9	0.693	0.7331
	307.9	0.690	0.7331
	333.0	0.486	0.7064
	333.0	0.486	0.7064
	347.3	0.417	0.6907
	347.3	0.420	0.6907
	373.0	0.298	0.6614
	373.0	0.298	0.6614
	405.3	0.207	0.6216
	420.8	0.184	0.6013
	426.4	0.166	0.5937
	441.7	0.142	0.5725
	441.7	0.140	0.5725
	464.9	0.129	0.5386
	474.3	0.104	0.5244
	496.3	0.089	0.4903
0.9	293.2	0.979	0.7659
	304.7	0.821	0.7534
	352.9	0.430	0.6989
	395.7	0.250	0.6458
	415.6	0.199	0.6189
	453.1	0.132	0.5643
	495.6	0.087	0.4968
	505.6	0.086	0.4804

range (*23*). An attempt to fit the data with an empirical Andrade correlation, which has the general form

$$\ln(\nu) = \ln(A) + B/T \qquad (13)$$

proved inadequate for the wide temperature range of the study. The correlation shown in Figure 3 includes only the data below the normal boiling point. The curvature of the relationship near the critical point indicates that a more complex relationship is necessary to describe the data. Reid, Sherwood, and Prausnitz (*17*) recommend a three-constant equation of the Antoine equation form. With the data at hand, this correlation gave physically unreasonable constants. The limited success encountered in predicting liquid viscosity over the temperature range between the melting point and the critical point is the direct result of inadequacies in the theory of the liquid state.

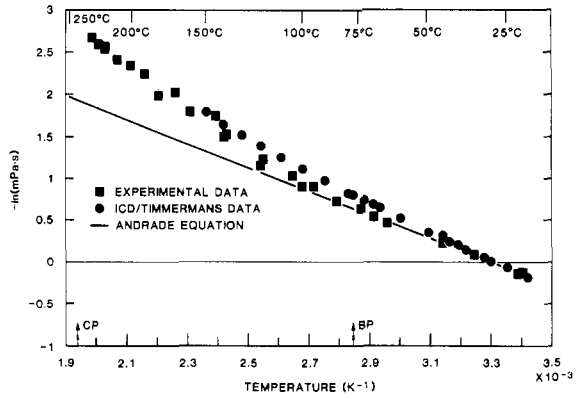

Figure 3. Viscosity of pure ethanol for the temperature range 20–230 °C.

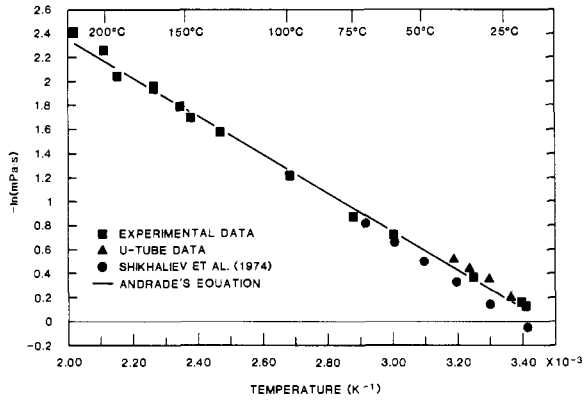

Figure 4. Mixture viscosity data for a typical ethanol (x = 0.8)–n-heptane mixture over the temperature range of the study.

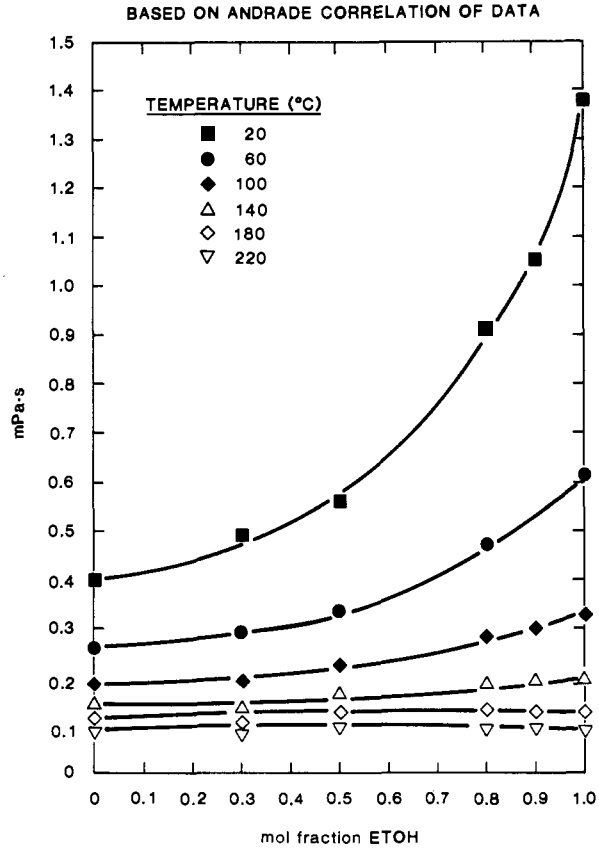

Figure 5. Mixture viscosity data for all ethanol–n-heptane mixtures over the temperature range of the study. Isotherms computed from Andrade constants derived from raw data.

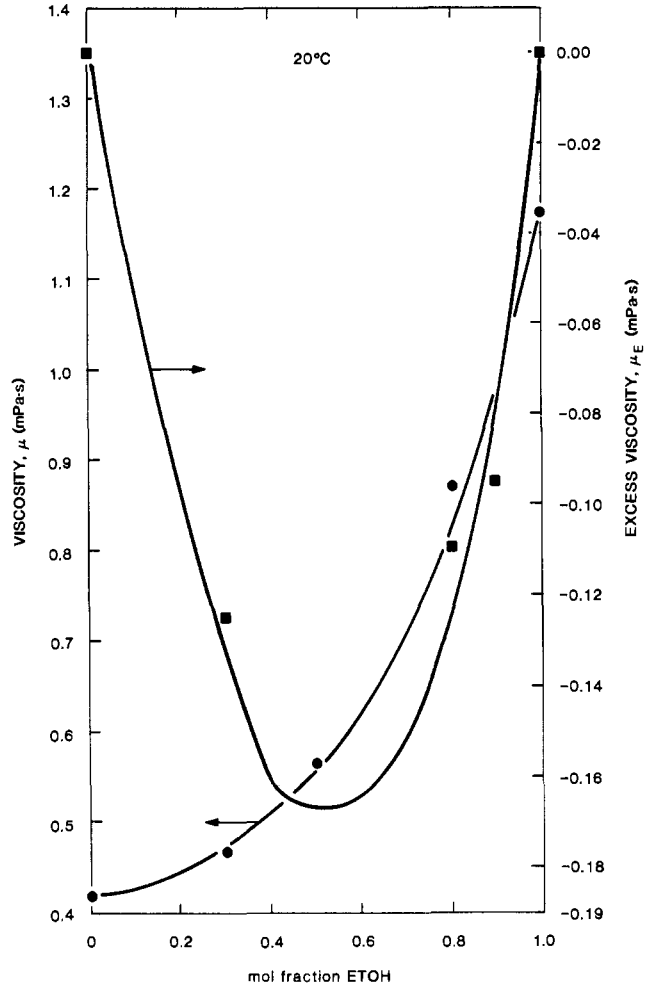

Figure 6. Viscosity and excess viscosity of the ethanol–n-heptane system at 20 °C.

Viscosities of Mixtures. Binary liquid mixtures of ethanol and n-heptane were studied over the entire composition range and from room temperature to 210 °C. Again the laser light scattering results were verified by low-temperature capillary viscometer measurements, which are reported in Table V. The laser light scattering results are reported in Table VI. The stability of the mixtures varied from high stability in the predominantly ethanol mixtures to lower stability in those containing primarily n-heptane. Mixing the second component into the pure material containing the silica particles did not appear to destabilize the suspension.

The temperature variations of a typical mixture (0.8 mole fraction ethanol) are shown as an Arrhenius plot in Figure 4. In this case the Andrade correlation gave a good fit to the data over the entire temperature range. The primary reason for exhibiting the particular mixture is that it affords an opportunity to compare our data acquired by capillary viscometer and by laser light scattering with the single set of data which are available in the literature (*24*). While our two measurements agree closely, the previous result is in substantial disagreement with the current data, particularly at room temperature. The other mixture data which we acquired produced curves similar to those in Figure 5.

On the basis of the series of Andrade correlations for different concentrations, it was possible to produce the isothermal viscosity–mole fraction curves in Figure 5. Because the data for different mole fractions were taken at slightly different temperatures, it was necessary to correct each point by using an Andrade correlation to a uniform temperature (e.g., 60 °C). The data showed a pronounced concave functionality indicating re-

pulsion of the two species. This contention is reinforced by the excess viscosity curve for 25 °C which is given in Figure 6. The extreme negative excess viscosity of 0.17 mPa·s represents a moderate repulsion (*11*). This is probably caused by the disruption of the hydrogen-bonding network which results from mixing the *n*-heptane in ethanol.

Conclusions

A rapid reliable method of measuring viscosities of liquids and liquid mixtures by use of laser light scattering has been tested in the region between the normal boiling point and the critical point. While the silica particles which are suspended in the liquid exhibit different stabilities, all allow the measurement of viscosities well above the normal boiling point. In the case of ethanol we were able to measure viscosities within 13 °C of the critical point.

Pure viscosities of both hydrocarbons and alcohols are not well fitted by an Andrade correlation over the broad temperature range of this study. A three-parameter equation, such as an Antoine-type correlation, is required.

Alcohol–hydrocarbon mixtures exhibit significant negative deviations from ideality, indicating that the hydrogen-bonding network is disturbed by the presence of the hydrocarbon in the alcohol matrix. As temperature rises, this effect substantially subsides because of the increasing significance of the kinetic energy.

Acknowledgment

The help and suggestions of Michael Harris and David Williams during the experimental program and while the paper was in preparation are appreciated.

Glossary

a	particle radius
A	Andrade coefficient, mPa·s (cP)
$A(t)$	arbitrary signal, continuous function of time
$\bar{A}(t)$	fluctuating influence of molecular collisions on particle motion
$A_s^*(\tau)$	time domain autocorrelation function of $A(t)$ (heterodyne)
$A^*(\omega)$	frequency domain scattering results
B	Andrade coefficient, K
d_p	particle diameter
D	self-diffusion coefficient = $kT/(6\pi a\eta)$
$f(r)$	normal distribution of particles
k	Boltzmann constant
K	arbitrary constant
K_E	kinetic energy correction constant
L	viscometer tube length, m
m	particle mass
M	molecular weight
n	medium refractive index
N	number of particles in scattering volume
P	pressure, Pa
$P(q,r)$	Mie scattering factor
$\bar{q}$	scattered field vector = vector difference between incident and scattered propagation vectors
$\bar{r}$	position vector
R	tube radius, m
t	time, s
T	temperature (absolute)
$\bar{u}$	velocity vector
V	mole volume, m^3/mol
v	volume, m^3
x	mole fraction
z	average hydrostatic level, m

Greek Letters

β	coefficient of dynamic friction $\sim 6\pi a\eta/m$
Γ	line width (Hz), half-width at half-height of frequency domain autocorrelation function $\sim q_2D$ (heterodyne case) or $\sim 2q_2D$ (homodyne)
Δ	change in (e.g., ΔP = pressure change)
η	shear viscosity
θ	scattering angle
λ	wavelength of light
μ_n	moment of distribution, order n
μ	dynamic viscosity, mPa·s
ν	kinematic viscosity, mm^2/s
ρ	fluid density, kg/L
τ	time increment
τ_c	characteristic decay time of autocorrelation function
ω	acentric factor

Subscripts

c	critical point
C	calibration constant
E	excess viscosity property
i, j	refers to components i, j
m	mixture
o	initial or original condition
r	reduced
s	scattered condition

Superscripts

°	referring to an ideal mixture
0	at zero pressure
R	at the reference point
L	of mixture

Registry No. Ethanol, 64-17-5; 1-butanol, 71-36-3; heptane, 142-82-5.

Literature Cited

(1) Berne, B. J.; Pecora, R. *Dynamic Light Scattering*; Wiley: New York, 1976.
(2) Dahneke, B., Ed. *Measurement of Suspended Particles by Quasi-Elastic Light Scattering*; Wiley: New York, 1983.
(3) Williams, D. F.; Byers, C. H. *J. Phys. Chem.* **1986**, *90*, 2534.
(4) Chandrasekhar, S. *Rev. Mod. Phys.* **1943**, *15*, 1.
(5) Crosignoni, B.; Di Porto, P.; Bertolotti, M. *Statistical Properties of Scattered Light*; Academic: New York, 1974.
(6) Chu, B. *Laser Light Scattering*; Academic: New York, 1974.
(7) Provencher, S. W. *Makromol. Chem.* **1979**, *180*, 201.
(8) Brown, J. C.; Pausey, P. N. *J. Chem. Phys.* **1975**, *62*, 1136.
(9) Bargeron, C. B. *J. Chem. Phys.* **1975**, *61*, 2134.
(10) Koppel, D. E. *J. Chem. Phys.* **1972**, *57*, 4184.
(11) Byers, C. H.; Williams, D. F. *J. Chem. Eng. Data* **1987**, *32*, 349.
(12) Williams, D. F.; Byers, C. H.; Young, C. R. *Viscosities of Polyaromatic Hydrocarbons: Experiment and Prediction*; ORNL/TM-9410; Oak Ridge National Laboratory: Oak Ridge, TN, 1985.
(13) Williams, D. F. *Determination of High-Temperature Fluid Viscosity Using Dynamic Light Scattering*; M.S. Thesis, University of Tennessee, Knoxville, TN, 1985.
(14) Saad, H.; Gulari, E. *J. Phys. Chem.* **1984**, *88*, 136–139.
(15) Byers, C. H.; Williams, D. F. *J. Chem. Eng. Data* **1987**, *32*, 344.
(16) Gunn, R. D.; Yamada, T. *AIChE J.* **1971**, *17*, 1341.
(17) Reid, R. C.; Prausnitz, J. M.; Sherwood, T. K. *The Properties of Gases and Liquids*; McGraw-Hill: New York, 1977.
(18) Lymans, W. J., et al. *Handbook of Chemical Property Estimation Methods*; McGraw-Hill: New York, 1977; Chapter 26.
(19) Van Helden, A. K., et al. *J. Colloid Interface Sci.* **1981**, *81*, 354–368.
(20) Stober, W., et al. *J. Colloid Interface Sci.* **1988**, *26*, 62–69.
(21) Iler, R. K. *Surface Colloid Sci.* **1973**, *6*, 77.
(22) Deglorgio, V.; Lastokova, J. B. *Phys. Rev. A* **1971**, *4*, 2033–2050.
(23) Timmermans, T. *Physico-Chemical Constants of Pure Organic Compounds*; Elsevier: New York, 1950.
(24) Shikhaliev, et al. *Russ. J. Phys. Chem.* **1974**, *48*, 1002–1004.

Received for review January 15, 1988. Accepted August 5, 1988. This research was sponsored by the Office of Basic Energy Sciences, U.S. Department of Energy, under Contract No. DE-AC05-84OR21400 with Martin Marietta Energy Systems, Inc.